



# General Framework for Mimetic Differences

Miguel A. Dumett and Jose E. Castillo

June 25, 2024

Publication Number: CSRCR2024-07

Computational Science &  
Engineering Faculty and Students  
Research Articles

Database Powered by the  
Computational Science Research Center  
Computing Group & Visualization Lab

# COMPUTATIONAL SCIENCE & ENGINEERING



**SAN DIEGO STATE  
UNIVERSITY**

Computational Science Research Center  
College of Sciences  
5500 Campanile Drive  
San Diego, CA 92182-1245  
(619) 594-3430



# General Framework For Mimetic Differences

Miguel A. Dumett \*      Jose E. Castillo†

June 25, 2024

## Abstract

In this work, it is demonstrated that mimetic difference schemes, of arbitrary order of accuracy, preserve energy and mass for general systems of conservation laws. This is shown by utilizing a framework that encompasses all mimetic difference approaches.

## 1 Introduction

Traditional discretization techniques for the numerical solution of partial differential equations (PDEs) include finite difference methods [1, 2, 3, 4], finite volume method [5], finite element method [6], as well as others. Besides convergence, and order of accuracy, one would expect the numerical solution of any method to replicate in the discrete realm some of the properties that the exact solution of the continuum model exhibit. Along this line, mimetic methods aim to satisfy, in the discrete sense, properties that the continuum equations hold. What are the features that the discrete solution should display and what the relationships that the discrete analogs of the differential operators have to reproduce, are the reason that have triggered the evolution of the different mimetic methods.

Initially, mimetic techniques were derived from enforcing certain vector calculus integral theorems or Green's identities derived from the different differentiation of product rules [7, 8, 9, 10]. From these starting points, they are able to mimic in the discrete, solution symmetries, conservation laws, and other important properties of continuum PDE mathematical models as well as vector calculus identities. For example, the mimetic difference (MD) [8, 10] approaches aim to replicate the extended Gauss Divergence Theorem.

Later, mimetic approaches that target to create a discrete calculus that replicates the continuum relationships of one among vector, tensor, exterior, calculi, were considered. The procedures in this last category are called fully mimetic. Examples of methods that elaborate a discrete vector calculus [11], tensor calculus [9, 12], exterior calculus [13, 14, 15], and others based on algebraic topology [16, 17], as well as geometric and structure-preserving methods [18], can be found in the literature.

The original versions of the mimetic methods that attain properties from some integral theorem, were restricted to be of low-order of accuracy [7], and it was demonstrated that utilizing the standard finite dimensional inner product, it cannot be possible to replicate integral theorems with high-order accuracy [19]. To remedy this situation, the first method to construct high-order operators was later introduced in [8]. It utilizes appropriate generalized inner products to enforce a discrete high-order accurate extended Gauss divergence theorem, by considering neighboring cells. Later, other

---

\*Computational Science Research Center at San Diego State University (mdumett@sdsu.edu).

†Computational Science Research Center at San Diego State University (jcastillo@sdsu.edu).

methods were able to do so, but by increasing the degree of the polynomials that approximate the exact solution on each cell, in this way increasing substantially the number of degrees of freedom of the discrete problem. Nevertheless, a feature of MD approaches that no other method, whether mimetic or not, is able to reproduce, so far, is the uniform accuracy they achieve over the whole computational domain (including near boundary grid points).

This document proceeds in the following way. Section 2 introduces a general frame for constructing MD approaches without ever specifying its building blocks. It also exhibits basic properties that the general MD framework holds. In other words, instead of deriving mimetic properties from given gradient and divergence discrete analogs, this work establishes a new derivation of mimetic differences from just the discrete analog of the integration by parts (IBP) formula in one-dimension, without ever specifying the gradient and divergence discrete analogs.

From it, all properties that mimetic difference operators gradient, divergence, as well as quadrature weights, should hold are obtained. Consequences of these basic identities such vector calculus identities, quadratures properties, and mass and energy conservation of mimetic schemes, can be easily attained. Sections 3 introduces examples of operators for different mimetic difference approaches. This new frame removes several intrinsic limitations that that mimetic differences exhibit and it is a step forward to demonstrate that MD approach features can indeed be inferred from the just a discrete analog of the extended Gauss Divergence Theorem.

Section 4 provides some conclusions.

## 2 A new frame for high-order mimetic differences

The following is a new way of presenting the derivation of MD approaches. It focuses on the discrete analog of the IBP formula, and obtains the main properties of the one-dimensional (1D) operator discrete analogs without explicitly finding them. These properties replicate in the discrete realm the Fundamental Theorem of Calculus (FTC).

### 2.1 One-dimensional mimetic differences

The general frame for MD approaches is introduced for 1D first.

#### 2.1.1 The staggered grid

In  $[-1, 1]$ , MD utilizes a mesh of  $N$  uniform cells and a staggered grid. The staggered grid is composed of a face grid that contains the edges of the cells (or nodes)

$$X_F = \left\{ x_l = -1 + \frac{2l}{N}, 0 \leq l \leq N \right\},$$

and a center grid, that includes all center cells and domain boundary points,

$$X_C = \{-1\} \cup \left\{ x_{l+\frac{1}{2}} = -1 + \frac{1}{N} + \frac{2l}{N}, 0 \leq l \leq N-1 \right\} \cup \{1\}.$$

Notice that the cardinalities of both  $X_F$  and  $X_C$  are different.

Neumann boundary conditions require that the gradient of boundary points should be calculated. On the other hand, the definition of the divergence, as a limit of a quotient of a flux (given by a surface integral) and the corresponding surface area when the region volume goes to zero, points

toward the lack of sense of computing the divergence of boundary points. Furthermore, gradients operate on scalar fields and return vector fields, while divergences act on vector fields and output scalar fields.

This complementary nature suggests that discrete scalar fields should be defined on centers or boundaries and discrete vector fields on edges. Moreover, one could argue that gradient  $G$ , and divergence  $D$ , discrete analogs should be mappings such  $G : X_C \rightarrow X_F$ ,  $D : X_F \rightarrow X_C$ . Therefore the non-square matrix representations of  $G$  and  $D$  are of orders  $(N+1) \times (N+2)$  and  $(N+2) \times (N+1)$ , respectively.

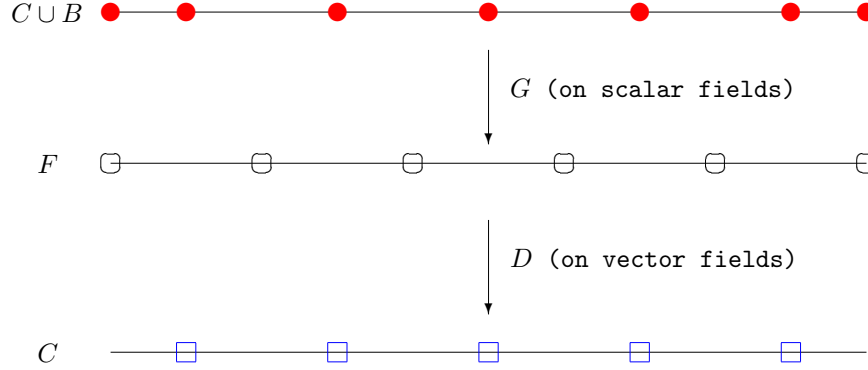


Figure 1:  $C$  centers,  $F$  faces (or edges) and  $B$  boundary.

In addition, since the gradient of a scalar constant field should be the zero vector field, discretization of this property imposes that if  $G = [G_{ij}]$ ,  $1 \leq i \leq N + 1$ ,  $1 \leq j \leq N + 2$ , then  $G\mathbf{1} = \vec{0}$ , where  $\mathbf{1} = (1, \dots, 1) \in \mathbb{R}^{N+2}$ , or equivalently,

$$\sum_{j=1}^{N+2} G_{ij} = 0, \quad 1 \leq i \leq N + 1. \quad (1)$$

Similarly, the divergence of a constant vector field is zero and

$$\sum_{j=1}^{N+1} D_{ij} = 0, \quad 1 \leq i \leq N + 2, \quad (2)$$

with the caveat that the first and last rows of  $D$  are zero since it does not have sense to compute the divergence at boundary points.

The Laplacian discrete analog  $L = DG \in \mathbb{R}^{(N+2) \times (N+2)}$  is defined as the product of divergence and the gradient, mimicking the fact that the Laplacian is the divergence of the gradient and its matrix representation should be given as the product of the matrix representations of the divergence and the gradient, respectively.

Moreover, MD operators are chiefly constructed to approximate with high accuracy the integration by parts formula (IBP) for 1D scalar field  $f$  and 1D vector field  $\vec{v}$ ,

$$\int_U \vec{v} \cdot \nabla f \, dU + \int_U f \nabla \cdot \vec{v} \, dU = \int_{\partial U} f \vec{v} \cdot \vec{n} \, dS. \quad (3)$$

The high-order discrete IBP formula requires that

$$\langle DV, F \rangle + \langle V, GF \rangle = V_N F_N - V_0 F_0,$$

where  $V = v|_{x_F}, F = f|_{x_C}$ , are the projections of  $v, f$  to the finite grids, respectively, and the angular brackets mean that the integrals are approximated utilizing a classic quadrature. However, this is not possible to achieve [19] unless special weighted inner products are introduced, meaning the need of MD diagonal weights  $P \in \mathbb{R}^{(N+1) \times (N+1)}$  and  $Q \in \mathbb{R}^{(N+2) \times (N+2)}$ , such the following identity is attained with high-order accuracy,

$$\langle DV, F \rangle_Q + \langle V, GF \rangle_P = V_N F_N - V_0 F_0. \quad (4)$$

If in (4), one assumes the constant scalar field  $F = \mathbf{1} \in \mathbb{R}^{(N+2) \times 1}$ , then (1) implies

$$h \langle DV, \mathbf{1} \rangle_Q = V_N - V_0. \quad (5)$$

Notice that (5) is the FTC discrete analog for 1D vector fields.

In addition, (5) can also be written as

$$h \mathbf{1}^T (QD)V = V_N - V_0. \quad (6)$$

Since  $\langle DV, \mathbf{1} \rangle_Q = \langle QDV, \mathbf{1} \rangle = \langle V, D^T Q \mathbf{1} \rangle = V^T D^T Q \mathbf{1}$ , then for all  $V$ , (5) becomes

$$h V^T D^T Q \mathbf{1} = V^T (-1, 0, \dots, 0, 1)^T,$$

or equivalently, since for  $q = (q_1, \dots, q_{N+2})^T$  and  $Q = \text{diag}(q)$ , one has that  $\mathbf{1}^T Q = q^T$ , and if  $b_{N+1} = (-1, 0, \dots, 0, 1) \in \mathbb{R}^{1 \times (N+1)}$ , one gets

$$h D^T q = b_{N+1}^T. \quad (7)$$

System (7) is utilized to find  $Q$ , once  $D$  is defined.

A similar argument can be given for  $P$ .

If in (4), one assumes the constant vector field  $V = \mathbf{1} \in \mathbb{R}^{(N+1) \times 1}$ , then (2) implies

$$h \langle GF, \mathbf{1} \rangle_P = F_{N+1} - F_0. \quad (8)$$

Observe that (8) is the FTC discrete analog for 1D scalar fields.

Equation (8) can also be written as

$$h \mathbf{1}^T (PG)F = F_{N+1} - F_0, \quad (9)$$

and  $\langle GF, \mathbf{1} \rangle_P = \langle PGF, \mathbf{1} \rangle = \langle F, G^T P \mathbf{1} \rangle = F^T G^T P \mathbf{1}$ , and for all  $F$  implies

$$h F^T G^T P \mathbf{1} = F^T (-1, 0, \dots, 0, 1)^T,$$

or equivalently, for  $p = (p_1, \dots, p_{N+2})^T$  and  $P = \text{diag}(p)$ , one has that  $\mathbf{1}^T P = p^T$ , and if  $b_{N+2} = (-1, 0, \dots, 0, 1) \in \mathbb{R}^{1 \times (N+2)}$  then

$$h G^T p \mathbf{1} = b_{N+2}^T, \quad (10)$$

which is utilized to find  $P$  once  $G$  is defined.

Since the first and last rows of  $D$  are zero, the number of equations of linear systems (7) and (10) exceeds by one the number of unknowns. Nevertheless, if one introduces some symmetry and structure to discrete analogs  $G$  and  $D$ , it is possible to show that systems (7) and (10) decouple, and that the number of constraints reduces below the number of degrees of freedom of  $p$  and  $q$ .

Sets	Description	Stencils	Band Size
$X_0^k$	Uses $x_0$	$S_0^k$	$\bar{b}$
$Y_0^k$	Uses interior in $S_0^k$	$S^k$	$b$
$Z^k$	Uses interior not in $S_0^k$	$S^k$	$b \geq k$
$Y_N^k$	Uses interior in $S_N^k$	$S^k$	$b$
$X_N^k$	Uses $x_N$	$S_N^k$	$\bar{b} > k$

Table 1: Stencils of order  $k$

### 2.1.2 Adding structure to $G$ and $D$

In terms of speeding up and simplify computations one would like to work with sparse matrices.

To understand how this reduction of constraints can be done with sparse matrices, consider the following splitting of the grid points  $X_F \cup X_C = X_F \sqcup (X_C \setminus B)$ , where  $B = \{x_0, x_N\}$  is composed of the two vertices, and  $\sqcup$  stands for the disjoint union.

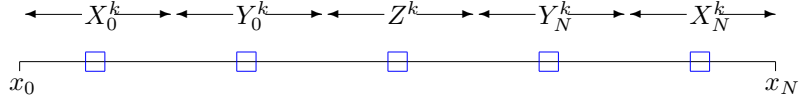


Figure 2: Grid splitting.

First-order derivatives are calculated on the range  $\mathcal{R}$  of the discrete operator utilizing its discrete domain  $\mathcal{D}$ . For an operator (divergence  $D$  or gradient  $G$ ) of accuracy order  $k$ , the set  $\mathcal{R}^k$  will be split into disjoint subsets  $X_0^k, Y_0^k, Z^k, Y_N^k, X_N^k$ , where

- $X_0^k$  are the points of  $\mathcal{R}^k$ , where the computation of the  $k$ -accurate first-order partial derivative utilizes the left boundary point  $x_0$ . All points in  $X_0^k$  will use by definition, (potentially) the same stencil  $S_0^k$  (of cardinality  $\bar{b}_0$ ) of input data points in  $\mathcal{D}$  that are close to  $x_0$  (including it by definition).
- Similarly all points in  $X_N^k$  with respect to the right boundary point  $x_N$  will have stencil  $S_N^k$  (of cardinality  $\bar{b}_N$ ).
- $Z^k$  are the points, whose stencils do not utilize any of the points in  $S_0^k \cup S_N^k$ . Its stencil has a band  $b$ . For any point  $x_i \in Z^k$ , it is assumed that its stencil is  $S^k$  (independent of  $x_i$ ) of even band size  $b$ , is symmetric with respect to  $x_i$  and that the stencil weights are anti-symmetric, i.e., for points  $x_j, x_l \in S^k$ , that are symmetric with respect to  $w_i$ , the sum of the corresponding weights is zero.
- $Y_0^k$  are the remaining points in  $\mathcal{R}^k$  that are closer to  $x_0$  than to  $x_N$ . The stencil of this points do not contain  $x_0$ . For simplicity, assume that the stencil weights of  $Y_0^k$  is given by  $S^k$ .
- Similarly, is defined  $Y_N^k$  with respect to  $x_N$ , instead of  $x_0$ .

The description of the stencils of the different sets of grid points  $\mathcal{R}^k$ , where the first-derivatives are computed, utilizing data points from  $\mathcal{D}^k$  are summarized in Table 1.

The partition of  $\mathcal{R}^k$  introduces a partition of the discrete analogs of  $D$ , given by

$$\begin{array}{l} X_0^k \rightarrow \\ Y_0^k \rightarrow \\ Z^k \rightarrow \\ Y_N^k \rightarrow \\ X_0^k \rightarrow \end{array} \left[ \begin{array}{c|c|c} D_{X_0^k} & & \\ \hline D_{Y_0^k} & & \\ \hline & D_{Z^k} & \\ \hline & & D_{Y_N^k} \\ \hline & & D_{X_N^k} \end{array} \right]$$

where and similarly for  $G$ .

Notice that by construction  $D_{Z^k}$  is an anti-symmetric matrix, i.e.,  $D_{Z^k} = -D_{Z^k}^T$ . In particular, the row and column sums of  $D_{Z^k}$  are zero.

One naturally introduces the center-skew-symmetric property for both  $D$  and  $G$ , which means that

$$D_{X_N^k} = -D_{X_0^k}^F, \quad D_{Y_N^k} = -D_{Y_0^k}^F, \quad G_{X_N^k} = -G_{X_0^k}^F, \quad G_{Y_N^k} = -G_{Y_0^k}^F,$$

where the upper index  $F$  is the operation that flips a matrix around its columns followed by a flip of its rows. These properties followed if one requires that the stencil weights for points close to one boundary should be a reflection of the stencil weights of points close to the other boundary.

Observe that the center-skew-symmetry property imposes that  $\bar{b}_0 = \bar{b}_N = \bar{b}$ , and that  $D_{Z^k} \in \mathbb{R}^{N+2-2\bar{b}}$ , where  $r$  is the number of rows of  $D$ . Similarly for  $G$ .

The splitting of  $D$  and  $G$ , triggers the following decomposition of matrices  $Q$  and  $P$ , respectively

$$Q = \left[ \begin{array}{c|c|c} Q_0^k & & \\ \hline & I_{N+2-2\bar{b}} & \\ \hline & & Q_N^k = (Q_0^k)^F \end{array} \right], \quad P = \left[ \begin{array}{c|c|c} P_0^k & & \\ \hline & I_{N+1-2\bar{b}} & \\ \hline & & P_N^k = (P_0^k)^F \end{array} \right],$$

where  $I_m$  is the identity matrix of order  $m$ .

The constraint reduction of systems (7) and (10) follows from the splitting of  $G$  and  $D$  above. Therefore, systems (7) and (10) reduce to  $k$  linear constraints and  $\bar{b} > k$  unknowns. If one writes  $P$  and  $Q$  weights as coefficients  $w_l$ ,  $l = 1, \dots, \bar{b}$ , one expects them to be positive. This can be enforced if utilizing the  $k$  reduced linear conditions in  $\bar{b}$  coefficients one writes each  $w_j$ ,  $j = \bar{b} - k + 1, \dots, \bar{b}$  in terms of  $w_i$ ,  $i = 1, \dots, \bar{b} - k$  and then impose the non-negative restrictions  $w_l \geq 0$ ,  $l = 1, \dots, \bar{b}$ . The collection  $\{w_l \geq 0\}$  will generate a convex polytope feasible region which is non-empty for large enough  $\bar{b}$ . Weights  $w_l$  can be arbitrarily selected from inside that regions. Boundary points have at least one  $w_l$  equal to zero and should be avoided. So, there are infinitely many solutions  $\{w_l \geq 0\}$ . Additional structure among coefficients  $w_l$  can be utilize to determine uniquely weights  $w_l$ .

## 2.2 Weights $Q$ and $P$ as high-order quadratures

One naturally wonders if non-negative weights  $\{w_l\}$  can be used for general quadratures in the sense of approximating  $\int_{x_0}^{x_N} g(x) dx$ , for a smooth function  $g$ , i.e.,

$$(1, \dots, 1)hWg \approx \int_{x_0}^{x_N} g(x) dx,$$

where  $g$  is the projection of the function  $g(x)$  onto a grid  $[x_0, x_1, \dots, x_N]$  and with  $W = P$ , or  $W = Q$ , with  $W = \text{diag}(W_L, I, W_R)$ ,  $W_L = \text{diag}(w_1, \dots, w_{\bar{b}})$ ,  $W_R = \text{diag}(w_{\bar{b}}, \dots, w_1)$  and  $I$  an appropriate square identity matrix.

Without loss of generality, one can assume enough differentiability for  $g$ , and hence there exist a smooth function  $G(x)$  such  $g(x) = G'(x)$ . In that case,

$$(1, \dots, 1)hWg \approx \int_{x_0}^{x_N} g(x) dx = \int_{x_0}^{x_N} G'(x) dx = G(x_N) - G(x_0). \quad (11)$$

Notice that formula (11) is verified by  $Q$  for vector fields  $V$  (see (6)) and satisfied by  $P$  for scalar fields  $F$  (see (9)).

### 2.3 Non-uniform grids

Constructing the divergence  $D_{nu}$  and the gradient  $G_{nu}$  operators for a non-uniform one-dimensional grid can be easily done if one has the non-uniform grid  $y = (y_1, \dots, y_m)^T$  and the uniform divergence  $D_u$  and gradient  $G_u$  operators [20, 21]. If  $h$  is the cell size in the one-dimensional uniform size, it can be shown that the non-uniform and gradient operators are given by

$$D_{nu} = h(\text{diag}(D_u y))^{-1} D_u, \quad G_{nu} = h(\text{diag}(G_u y))^{-1} G_u.$$

### 2.4 Some mimetic difference operator properties in $d$ -dimensions

In  $[-1, 1]^d$ , MD utilizes  $m_l$  cells along axis  $X_l$ ,  $l = 1, \dots, d$ . The staggered grid is composed of cell centers and cell vertices  $X_C$ , and of cell centered faces  $X_F$ , given respectively by

$$\begin{aligned} X_F &= \bigcup_{j=1}^d \left[ \left( \prod_{l < j} (X_C^j \setminus \{-1, 1\}) \right) \times X_F^j \times \left( \prod_{l > j} (X_C^j \setminus \{-1, 1\}) \right) \right], \\ X_C &= \prod_{j=1}^d X_C^j. \end{aligned}$$

Extensions of the 1D divergence  $D$ , gradient  $G$ , and inner product weight operators  $Q$  and  $P$  are built by utilizing Kronecker products of the 1D operators and some near identity of convenient orders. So, one has that the matrix representations of:

1. The discrete analogs of the order  $k$  divergence  $D_{x_1, \dots, x_d} : X_C \rightarrow X_F$ , is

$$\begin{aligned} D_{x_1, \dots, x_d}^{(k)} &= [D_{x_1, \dots, x_d, 1}^{(k)}, \dots, D_{x_1, \dots, x_d, d}^{(k)}] \\ &= [\hat{I}_{m_d} \otimes \dots \otimes \hat{I}_{m_2} \otimes D_{x_1}^{(k)}, \dots, D_{x_d}^{(k)} \otimes \hat{I}_{m_{d-1}} \otimes \dots \otimes \hat{I}_{m_1}], \end{aligned}$$

where  $D_{x_p}^{(k)}$  is the 1D divergence operator of accuracy order  $k$  along the  $p$ -axis, and

$$\hat{I}_q = \begin{bmatrix} 0_{1 \times q} \\ I_{q \times q} \\ 0_{1 \times q} \end{bmatrix}, \quad (12)$$

with  $I_{q \times q}$  is the  $q \times q$  identity matrix.

2. The discrete analogs of the order  $k$  gradient  $G_{x_1, \dots, x_d} : X_C \rightarrow X_F$ ,

$$G_{x_1, \dots, x_d}^{(k)} = \begin{bmatrix} G_{x_1, \dots, x_d, 1}^{(k)} \\ \vdots \\ G_{x_1, \dots, x_d, d}^{(k)} \end{bmatrix} = \begin{bmatrix} \hat{I}_{m_d}^T \otimes \dots \otimes \hat{I}_{m_2}^T \otimes G_{x_1}^{(k)} \\ \vdots \\ G_{x_d}^{(k)} \otimes \hat{I}_{m_{d-1}}^T \otimes \dots \otimes \hat{I}_{m_1}^T \end{bmatrix},$$

where  $G_{x_p}^{(k)}$  is the 1D gradient operator of accuracy order  $k$  along the  $p$ -axis.

3. The mimetic discrete inner product weight operators  $Q_{x_1, \dots, x_d} \in \mathbb{R}^{|X_C| \times |X_C|}$ , where  $|X_C| = \prod_{j=1}^d (m_j + 2)$ , is the cardinality of  $X_C$ ,

$$Q_{x_1, \dots, x_d}^{(k)} = \begin{bmatrix} I_{m_d+2} \otimes \dots \otimes I_{m_2+2} \otimes Q_{m_1+2}^{(k)} & & \\ & \ddots & \\ & & Q_{m_d+2}^{(k)} \otimes I_{m_{d-1}+2} \otimes \dots \otimes I_{m_1+2} \end{bmatrix},$$

where  $Q_m^{(k)} \in \mathbb{R}^{m \times m}$  is the 1D inner product weight  $Q$  of accuracy order  $k$ .

4. The mimetic discrete inner product weight operators  $P_{x_1, \dots, x_d} \in \mathbb{R}^{|X_F| \times |X_F|}$ , where  $|X_F| = \sum_{j=1}^d (m_j + 1) \prod_{l \neq j} m_l$ , is the cardinality of  $X_F$ ,

$$P_{x_1, \dots, x_d}^{(k)} = \begin{bmatrix} I_{m_d+2} \otimes \dots \otimes I_{m_2+2} \otimes P_{m_1+1}^{(k)} & & \\ & \ddots & \\ & & P_{m_d+1}^{(k)} \otimes I_{m_{d-1}+2} \otimes \dots \otimes I_{m_1+2} \end{bmatrix},$$

where  $P_m^{(k)} \in \mathbb{R}^{m \times m}$  is the 1D inner product weight  $P$  of accuracy order  $k$ .

In  $d$ -dimensions,  $d > 1$ , there are different partial derivatives. For the gradient, each of them is approximated at exactly one of the faces of the hyper-cube  $[-1, 1]^d$ . Similarly, for the divergence, each component takes its input from a different face of  $[-1, 1]^d$ . Since scalar fields defined on  $[-1, 1]^d$  are defined at centers, then different quantities may be at different set of points making difficult to compute their product in the extension of the integration by part formula in  $d$ -dimensions. High-order interpolation to move the data from one set of points to another are needed.

The  $d$ -dimension versions of them are defined also by Kronecker products between the corresponding 1D interpolation version and some identity matrices. They are given by

1. Interpolations from  $X_C$  to  $X_F$  given by

$$\begin{aligned} (I^D)_{x_1, \dots, x_d}^{(k)} &= \begin{bmatrix} (I^D)_{x_1, \dots, x_d, 1}^{(k)} & & \\ & \ddots & \\ & & (I^D)_{x_1, \dots, x_d, d}^{(k)} \end{bmatrix} \\ &= \begin{bmatrix} \hat{I}_{m_d}^T \otimes \dots \otimes \hat{I}_{m_2}^T \otimes (I^D)_{x_1}^{(k)} & & \\ & \ddots & \\ & & (I^D)_{x_d}^{(k)} \otimes \hat{I}_{m_{d-1}}^T \otimes \dots \otimes \hat{I}_{m_1}^T \end{bmatrix}, \end{aligned}$$

where  $(I^D)_{x_p}^{(k)}$  is the 1D interpolation operator from  $X_C^p$  to  $X_F^p$  of accuracy order  $k$  along the  $p$ -axis.

2. Interpolations from  $X_F$  to  $X_C$  given by

$$\begin{aligned} (I^G)_{x_1, \dots, x_d}^{(k)} &= \begin{bmatrix} (I^G)_{x_1, \dots, x_d, 1}^{(k)} & & \\ & \ddots & \\ & & (I^G)_{x_1, \dots, x_d, d}^{(k)} \end{bmatrix} \\ &= \begin{bmatrix} \hat{I}_{m_d} \otimes \dots \otimes \hat{I}_{m_2} \otimes (I^G)_{x_1}^{(k)} & & \\ & \ddots & \\ & & (I^G)_{x_d}^{(k)} \otimes \hat{I}_{m_{d-1}} \otimes \dots \otimes \hat{I}_{m_1} \end{bmatrix}, \end{aligned}$$

where  $(I^G)_p^{(k)}$  is the 1D interpolation operator from  $X_F^p$  to  $X_C^p$  of accuracy  $k$  along the  $p$ -axis.

The extension of the 1D integration by parts formula to  $d$ -dimension is called the extended Gauss divergence theorem. The discrete analog of the extended Gauss divergence theorem, neglecting the order of accuracy  $k$ , reads

$$\left( \prod_{l=1}^d \Delta x_l \right) \langle P_{x_1, \dots, x_d} G_{x_1, \dots, x_d} F, \vec{V} \rangle + \left( \prod_{l=1}^d \Delta x_l \right) \langle Q_{x_1, \dots, x_d} F, D_{x_1, \dots, x_d} \vec{V} \rangle = F^T \bar{B}_{x_1, \dots, x_d} \vec{V},$$

where  $F$  is the projection onto  $X_C$  of scalar field  $f: \mathbb{R}^d \rightarrow \mathbb{R}$ ,  $\vec{V}$  is the projection onto  $X_F$  of vector field  $\vec{v}: \mathbb{R}^d \rightarrow \mathbb{R}^d$ , and boundary operator

$$\bar{B}_{x_1, \dots, x_d} = \begin{pmatrix} I_{m_d+2} \otimes \dots \otimes I_{m_2+2} \otimes \bar{B}_{x_1} & & \\ & \ddots & \\ & & \bar{B}_{x_d} \otimes I_{m_{d-1}+2} \otimes \dots \otimes I_{m_1+2} \end{pmatrix},$$

where  $\bar{B}_{x_p}$  is the one dimensional boundary

$$\bar{B}_{x_p} = \begin{pmatrix} -1 & 0 & \dots & 0 & 0 \\ 0 & 0 & \dots & 0 & 0 \\ \vdots & \vdots & \vdots & \vdots & \vdots \\ 0 & 0 & \dots & 0 & 0 \\ 0 & 0 & \dots & 0 & 1 \end{pmatrix},$$

matrix along the  $p$ -axis. It can be proven by a direct computation (see [22, pp. 11-13]) that for a discrete constant scalar field  $F$ , one obtains

$$\left( \prod_{l=1}^d \Delta x_l \right) D_{x_1, \dots, x_d}^T Q_{x_1, \dots, x_d} \mathbf{1} = \begin{pmatrix} \mathbf{1} \otimes \mathbf{1} \otimes b_{m_1+1} & & \\ & \ddots & \\ & & b_{m_d+1} \otimes \mathbf{1} \otimes \mathbf{1} \end{pmatrix}, \quad (13)$$

with  $b_m = [-1, 0, \dots, 0, 1] \in \mathbb{R}^m$ .

## 2.5 Curvilinear structured grids

Extensions of the divergence and gradient operators to curvilinear structured meshes require the utilization of the Jacobians of transformations, which for staggered grids use interpolation operators intensively. We present only the 3D case, since the 2D case can be easily recovered from it.

### 2.5.1 The 3D case

This section introduces more detail the two ways of computing the spatial first-order partial derivatives that appear in the Jacobian computation according to the divergence or the gradient approach.

Suppose the curvilinear physical spatial domain  $\mathcal{P}$  in 3D, utilizes local coordinates  $x, y, z$ . Suppose  $\mathcal{P}$  is the result of a smooth bijection map  $\mathcal{X}$  given by

$$\begin{aligned} x &= x(\xi, \eta, \kappa) \\ y &= y(\xi, \eta, \kappa) \\ z &= z(\xi, \eta, \kappa), \end{aligned}$$

and that its inverse map is  $\Theta$ , given by

$$\begin{aligned} \xi &= \xi(x, y, z) \\ \eta &= \eta(x, y, z) \\ \kappa &= \kappa(x, y, z), \end{aligned}$$

maps  $\mathcal{P}$  onto a 3D logical Cartesian domain  $\mathcal{L}$ . If one defines a staggered grid on  $\mathcal{L}$  contains staggered grids  $X_F$  and  $X_C$ , then  $\mathcal{X}(X_C \cup X_F)$  is an structured grid on  $\mathcal{P}$ , with centers/boundaries  $\mathcal{C} = \mathcal{X}(X_C)$  and faces  $\mathcal{F} = \mathcal{X}(X_F)$ .

The Jacobian of the transformation  $\mathcal{X}$  is given by

$$J = \frac{\partial(x, y, z)}{\partial(\xi, \eta, \kappa)} = \begin{bmatrix} x_\xi & x_\eta & x_\kappa \\ y_\xi & y_\eta & y_\kappa \\ z_\xi & z_\eta & z_\kappa \end{bmatrix}.$$

A smooth function  $u : \mathcal{X} \rightarrow \mathbb{R}$ , with  $u = u(x, y, z) = u(x(\xi, \eta, \kappa), y(\xi, \eta, \kappa), z(\xi, \eta, \kappa))$ , can be seen as a function  $u = u(\xi, \theta, \kappa)$ , and the chain rule implies

$$\begin{aligned} u_\xi &= u_x x_\xi + u_y y_\xi + u_z z_\xi \\ u_\eta &= u_x x_\eta + u_y y_\eta + u_z z_\eta \\ u_\kappa &= u_x x_\kappa + u_y y_\kappa + u_z z_\kappa, \end{aligned}$$

or equivalently,

$$\begin{bmatrix} u_\xi \\ u_\eta \\ u_\kappa \end{bmatrix} = \begin{bmatrix} x_\xi & y_\xi & z_\xi \\ x_\eta & y_\eta & z_\eta \\ x_\kappa & y_\kappa & z_\kappa \end{bmatrix} \begin{bmatrix} u_x \\ u_y \\ u_z \end{bmatrix} = J^T \begin{bmatrix} u_x \\ u_y \\ u_z \end{bmatrix}.$$

Hence

$$\begin{bmatrix} u_x \\ u_y \\ u_z \end{bmatrix} = (J^T)^{-1} \begin{bmatrix} u_\xi \\ u_\eta \\ u_\kappa \end{bmatrix}.$$

Denote

$$J^T = \begin{bmatrix} \textcircled{1} := x_\xi & | & \textcircled{2} := y_\xi & | & \textcircled{3} := z_\xi \\ \textcircled{4} := x_\eta & | & \textcircled{5} := y_\eta & | & \textcircled{6} := z_\eta \\ \textcircled{7} := x_\kappa & | & \textcircled{8} := y_\kappa & | & \textcircled{9} := z_\kappa \end{bmatrix},$$

where circled numbers are defined (by the colon equal sign) to match some of the spatial derivatives of a physical quantity with respect to a logical coordinate. Since

$$\begin{bmatrix} a & b & c \\ d & e & f \\ g & h & i \end{bmatrix}^{-1} = \frac{1}{\Delta} \begin{bmatrix} ei - fh & ch - bi & bf - ce \\ fg - di & ai - cg & cd - af \\ dh - eg & bg - ah & ac - bd \end{bmatrix},$$

where  $\Delta = a(ei - fh) - b(di - fg) + c(dh - eg)$ , then

$$(J^T)^{-1} = \frac{1}{\Delta} \begin{bmatrix} \textcircled{5}\textcircled{9} - \textcircled{6}\textcircled{8} & \textcircled{3}\textcircled{8} - \textcircled{2}\textcircled{9} & \textcircled{2}\textcircled{6} - \textcircled{3}\textcircled{5} \\ \textcircled{6}\textcircled{7} - \textcircled{4}\textcircled{9} & \textcircled{1}\textcircled{9} - \textcircled{3}\textcircled{7} & \textcircled{3}\textcircled{4} - \textcircled{1}\textcircled{6} \\ \textcircled{4}\textcircled{8} - \textcircled{5}\textcircled{7} & \textcircled{2}\textcircled{7} - \textcircled{1}\textcircled{8} & \textcircled{1}\textcircled{5} - \textcircled{2}\textcircled{4} \end{bmatrix},$$

with

$$\Delta = \textcircled{1}(\textcircled{5}\textcircled{9} - \textcircled{6}\textcircled{8}) - \textcircled{2}(\textcircled{4}\textcircled{9} - \textcircled{6}\textcircled{7}) + \textcircled{3}(\textcircled{4}\textcircled{8} - \textcircled{5}\textcircled{7}).$$

The purpose of these definitions is to illustrate the need of interpolation operators to calculate the entries of the inverse Jacobian since each of the quantities shown is defined at different collection of points.

If one uses the gradient to approximate the partial derivatives of the Jacobian, then

$$J_G^T = I_{xyz}^{F \rightarrow C} \tilde{G}_{\xi\eta\kappa}$$

where  $I_{xyz}^{F \rightarrow C}$  is the 3D interpolation from faces to 3D centers,  $\tilde{G}_{xyz}$  is the same as  $G_{xyz}$  with  $\hat{I}_p$  (see (12)) replaced by  $I_{p+2}$ , the identity matrix of order  $p + 2$ .

If one computes the Jacobian at the centers then the physical gradient is given by

$$G_{xyz} = I_{xyz}^{C \rightarrow F} (J_G^T)^{-1} I_{\xi\eta\kappa}^{F \rightarrow C} G_{\xi\eta\kappa}.$$

Similarly, one can construct the Jacobian based on the divergence operator.

## 2.6 Vector Calculus identities

In [23], it is shown, without specifying  $D$  and  $G$ , that discrete analogs of vector calculus identities involving only the divergence and the gradient hold, in the integral sense, meaning that the integral version of the identities is replicated. This is because mimetic difference operators are constructed to satisfy the IBP formula, which is of integral nature.

## 2.7 General systems of conservation laws

Given the following sets

$$I = \{1, \dots, c\}, \quad J = \{1, \dots, d\}, \quad L = [-1, 1]^d, \quad L_0 = [-1, 1]^{d-1}, \quad K = [0, T],$$

consider the system of  $c$  conservation laws in  $d$ -dimensions, with  $x = (x_1, \dots, x_d)$ , and the unknown  $u(x, t) = (u_1(x, t), \dots, u_c(x, t))^T$ , and initial condition  $u^0(x) = (u_1^0(x), \dots, u_c^0(x))^T$ , that are described by

$$u_t + \text{div}(F(u)) = 0_{c \times 1}, \quad (x, t) \in \mathring{L} \times \mathring{K}, \quad (14)$$

$$u(x, 0) = u^0(x), \quad x \in L, \quad (15)$$

with  $\mathring{L} = \text{int}(L)$ , the interior of  $L$ , and that hold boundary conditions given by

$$\begin{aligned} u_i(x_1, \dots, x_{j-1}, -1, x_{j+1}, \dots, x_d, t) &= g_i^-(x_1, \dots, x_{j-1}, x_{j+1}, \dots, x_d, t), \quad i \in I, j \in J, \\ u_i(x_1, \dots, x_{j-1}, 1, x_{j+1}, \dots, x_d, t) &= g_i^+(x_1, \dots, x_{i-1}, x_{i+1}, \dots, x_d, t), \quad i \in I, j \in J, \end{aligned}$$

where  $g_i^\pm : L_0 \times K \rightarrow \mathbb{R}^c$ ,  $i = 1, \dots, c$ , are smooth functions. The flux  $F$  is given by

$$F(u) = \begin{pmatrix} F_{11}(u) & \cdots & F_{1d}(u) \\ \vdots & \ddots & \vdots \\ F_{c1}(u) & \cdots & F_{cd}(u) \end{pmatrix}.$$

Notice  $F_{ij} : \mathbb{R}^d \times \mathring{K} \rightarrow \mathbb{R}$ ,  $i \in I, j \in J$ . Denote  $F_i(u) = (F_{i1}(u), \dots, F_{id}(u))^T$ ,  $i \in I$ .

It can be shown that mimetic difference schemes preserve both mass and energy for systems of conservation laws. These will be proven in a future publication.

### 3 Examples

The following section shows a couple of realizations of the general framework.

#### 3.1 Castillo-Grone $D$ and $G$ operators

Castillo-Grone operators can be found in [21]. However, the reference has a series of typos difficult to find in some of the coefficients. Here, those typos are corrected.

##### 3.1.1 Divergence operators

For  $k = 2$ ,

$$D^{(2)} = \frac{1}{h} \begin{bmatrix} -1 & 1 & & & & & & & \\ & & \ddots & \ddots & & & & & \\ & & & & -1 & 1 & & & \\ & & & & & & & & \end{bmatrix}.$$

For  $k = 4$ ,

$$D^{(4)} = \frac{1}{h} \begin{bmatrix} -\frac{4751}{5192} & \frac{909}{1298} & \frac{6091}{15576} & -\frac{1165}{5192} & \frac{129}{2596} & -\frac{25}{15576} & 0 & \cdots \\ \frac{1}{24} & -\frac{9}{8} & \frac{9}{8} & -\frac{1}{24} & 0 & \cdots & & \\ & \ddots & \ddots & \ddots & \ddots & \ddots & & \end{bmatrix}.$$



For  $k = 4$ ,

$$G^{(4)} = \frac{1}{h} \begin{bmatrix} -\frac{1152}{407} & \frac{10063}{3256} & \frac{2483}{9768} & -\frac{3309}{3256} & \frac{2099}{3256} & -\frac{697}{4884} & 0 & \cdots \\ 0 & -\frac{11}{12} & \frac{17}{24} & \frac{3}{8} & -\frac{5}{24} & \frac{1}{24} & 0 & \cdots \\ 0 & \frac{1}{24} & -\frac{9}{8} & \frac{9}{8} & -\frac{1}{24} & 0 & \cdots \\ \vdots & \ddots \end{bmatrix}$$

For  $k = 6$ ,  $hG^{(6)}$  is given by

$$\begin{bmatrix} -\frac{568557184}{150834915} & \frac{455704609}{835795520} & -\frac{128942179}{417897760} & \frac{15911389}{6964960} & -\frac{142924471}{117011328} & \frac{20331719}{50147712} & -\frac{2688571}{38307280} & \frac{187529}{41789760} & -\frac{6207}{27859840} & 0 & \cdots \\ \frac{496}{3465} & -\frac{811}{640} & \frac{449}{384} & -\frac{29}{960} & -\frac{11}{448} & \frac{13}{1152} & -\frac{37}{21120} & 0 & \cdots \\ -\frac{8}{385} & \frac{179}{1920} & -\frac{153}{128} & \frac{381}{320} & -\frac{101}{1344} & \frac{1}{128} & -\frac{3}{7040} & 0 & \cdots \\ & -\frac{3}{640} & \frac{25}{384} & -\frac{75}{64} & \frac{75}{64} & -\frac{25}{384} & \frac{3}{640} & 0 & \cdots \\ & & \ddots \end{bmatrix}$$

For  $k = 8$ ,  $hG^{(8)}$  is given by

$$\begin{bmatrix} g_{1,1} & g_{1,2} & g_{1,3} & g_{1,4} & g_{1,5} & g_{1,6} & g_{1,7} & g_{1,8} & g_{1,9} & g_{1,10} & g_{1,11} & g_{1,12} & 0 & \cdots \\ \frac{86048}{675675} & -\frac{131093}{107520} & \frac{49087}{46080} & \frac{10973}{76800} & -\frac{4597}{21504} & \frac{4019}{27648} & -\frac{10331}{168960} & \frac{2983}{199680} & -\frac{2621}{1612800} & 0 & \cdots \\ -\frac{3776}{225225} & \frac{8707}{107520} & -\frac{17947}{15360} & \frac{29319}{25600} & -\frac{533}{21504} & -\frac{263}{9216} & \frac{903}{56320} & -\frac{283}{66560} & \frac{257}{537600} & 0 & \cdots \\ \frac{32}{9009} & -\frac{543}{35840} & \frac{265}{3072} & -\frac{1233}{1024} & \frac{8625}{7168} & -\frac{775}{9216} & \frac{639}{56320} & -\frac{15}{13312} & \frac{1}{21504} & 0 & \cdots \\ & \frac{5}{7168} & -\frac{49}{5120} & \frac{245}{3072} & -\frac{1225}{1024} & \frac{1225}{1024} & -\frac{245}{3072} & \frac{49}{5120} & -\frac{5}{7168} & 0 & \cdots \\ & & \ddots \end{bmatrix}$$

where

$$\begin{aligned} g_{1,1} &= \frac{375430666840256}{92579164853175}, & g_{1,2} &= \frac{46577871283831}{7366050101760}, & g_{1,3} &= \frac{44142164823881}{8839260122112}, \\ g_{1,4} &= \frac{50703079390921}{9207562627200}, & g_{1,5} &= \frac{71068924474957}{14732100203520}, & g_{1,6} &= \frac{57866887554917}{18941271690240}, \\ g_{1,7} &= \frac{30717060475411}{23150443176960}, & g_{1,8} &= \frac{2027314948429}{5471922932736}, & g_{1,9} &= \frac{13407250027393}{220981503052800}, \\ g_{1,10} &= \frac{82765484227}{14732100203520}, & g_{1,11} &= \frac{1177332481}{2455350033920}, & g_{1,12} &= \frac{21454295}{982140013568}. \end{aligned}$$

### 3.2 Corbino-Castillo $D$ and $G$ operators

Corbino-Castillo operators can be found in [23].

## 4 Conclusions

This document establishes a new frame for deriving all possible divergence and gradient operators for mimetic differences, as well as their corresponding quadratures. It is based on imposing structural properties and relationships among the different set of points that compose the computational grid. These relations are written in terms of stencils which provide a decomposition of both the divergence and the gradient matrix representations as well as their inner product weights.

## References

- [1] B. Gustafsson. *High Order Difference Methods for Time Dependent PDE*. Springer-Verlag, 2008.
- [2] M. A. Pinsky. *Partial Differential Equations and Boundary-Value Problems with Applications*. Mc Graw-Hill, 3rd edition edition, 1998.
- [3] J. W. Thomas. *Numerical Partial Differential Equations*. Springer-Verlag, 1995.
- [4] J. S. Hesthaven. *Numerical Methods for Conservation Laws*. SIAM, 2018.
- [5] R. J. LeVeque. *Finite volume methods for hyperbolic problems*. Cambridge University Press, 2002.
- [6] P. G. Ciarlet. *The Finite Element Method for Elliptic Problems*. SIAM, 2002.
- [7] M. Shashkov. *Conservative finite-difference methods on general grids*. CRC press, 1996.
- [8] J. E. Castillo and R. D. Grone. A matrix analysis approach to higher-order approximations for divergence and gradients satisfying a global conservation law. *SIAM Journal on Matrix Analysis and Applications*, 25(1):128–142, 2003.
- [9] L. B. da Veiga, K. Lipnikov, and G. Manzini. *The mimetic finite difference method for elliptic problems*. Springer, 2014.
- [10] J. Corbino and J. E. Castillo. High-order mimetic finite-difference operators satisfying the extended gauss divergence theorem. *Journal of Computational and Applied Mathematics*, 364:112326, 2020.
- [11] N. Robidoux and S. Steinberg. A discrete vector calculus in tensor grids. *Computational Methods in Applied Mathematics*, 11(1):23–66, 2011.
- [12] D. Justo. *High Order Mimetic Methods*. VDM Verlag Dr. Müller Aktiengesellschaft & Co. KG, 2009.
- [13] D. N. Arnold. *Finite Element Exterior Calculus*. SIAM, 2018.
- [14] J. Kreeft, A. Palha, and M. Gerritsma. Mimetic framework on curvilinear quadrilaterals of arbitrary order. *arXiv:1111.4304v1 [math.NA]*, 2011.
- [15] P. Bochev and Hyman J. M. Principles of mimetic discretizations of differential operators. In: *Arnold, D.N., Bochev, P.B., Lehoucq, R.B., Nicolaides, R.A., Shashkov, M. (eds) Compatible*

*Spatial Discretizations. The IMA Volumes in Mathematics and its Applications, Springer, New York, IMA vol. 142, 2006.*

- [16] C. Eldred and A. Salinger. Structure-preserving numerical discretizations for domains with boundaries. Technical Report SAND2021-11517, Sandia National Laboratories, September 2021.
- [17] C. Eldred and J. Stewart. Differential geometric approaches to momentum-based formulations for fluids. Technical Report SAND2022-12945, Sandia National Laboratories, September 2022.
- [18] H. Sharma, M. Patil, and C. Woolsey. A review of structure-preserving numerical methods for engineering applications. *Computer Methods in Applied Mechanics and Engineering*, 366(113067), 1 July 2020.
- [19] H-O. Kreiss and G. Scherer. Finite element and finite difference methods for hyperbolic partial differential equations. In *Mathematical aspects of finite elements in partial differential equations*, pages 195–212. Elsevier, 1974.
- [20] E. D. Batista and J. E. Castillo. Mimetic schemes on non-uniform structured meshes. *Electronic Transactions on Numerical Analysis*, 34(1):152–162, 2009.
- [21] J. E. Castillo and G. F. Miranda. *Mimetic Discretization Methods*. CRC Press, Boca Raton, Florida, USA, 2013.
- [22] M. A. Dumett and J. E. Castillo. Energy conservation and convergence of high-order mimetic schemes for the 3d advection equation. Technical report, San Diego State University, Computational Science Research Center, 07 2023.
- [23] M. A. Dumett and J. E. Castillo. Mimetic analogs of vector calculus identities. Technical report, San Diego State University, Computational Science Research Center, 07 2023.